*Progress In Electromagnetics Research Letters, Vol. 96, 53–58, 2021*

# Efficient Evaluation of the Time-Harmonic Response in Central Loop Electromagnetic Sounding

**Vincenzopio Tamburrelli[1] and Marcello Salis[2, *]**

**Abstract**—This work presents an efficient method that allows to accurately calculate the time-harmonic vertical magnetic field generated at the center of a large current-carrying coil of wire positioned above a layered ground. The method consists of evaluating the integral representation for the vertical magnetic field by using a hybrid procedure. At first, the direct and ideal reflected fields are extracted from the total magnetic field and expressed in explicit form. Then, the non-analytic part of the integrand of the remaining contribution is replaced with a sum of partial fractions, obtained by using a rational function fitting algorithm. Finally, the resulting sum of integrals is analytically evaluated and turned into a sum of modified Bessel functions of the second kind. The obtained expression for the magnetic field is then used to evaluate the voltage induced in a small receiving loop co-axial with the transmitting loop.

## 1. INTRODUCTION

Electromagnetic sounding is a well-known method of exploration of terrestrial areas, based on interpretation of measurements of the voltage induced in the receiver of a transmitter-receiver loop system [1–23]. In particular, information about the subsurface structure is acquired by solving the inverse problem of searching for the layered earth model that best matches the measurement data. Conventional iterative algorithms used for solving nonlinear inverse problems require the solution of a number of forward problems within an optimization loop [2, 4, 18]. Hence, the efficiency of the inversion procedure depends on that exhibited by the algorithm used for the calculation of the induced voltage and the generation of the theoretical response curves. In geophysical applications, it is a common practice to perform the measurements by positioning a small receiving loop at the center of a physically large transmitting loop. Yet, in spite of the widespread application of this technique, the problem of calculating the vertical magnetic field induced at the center of a large circular loop located above a layered earth is still far from being solved, and a solution can be derived only under the assumptions of single-layer ground and quasi-static field [10]. Except for that case, the radiated field and the voltage induced in the smaller loop can only be computed numerically, by resorting to integration techniques or simulations tools for solving EM boundary value problems [10, 23, 24].

This work presents an efficient hybrid analytical-numerical procedure for calculating the voltage response of a central-loop EM sounding system located above a layered medium. The procedure provides explicit expressions for the vertical magnetic field generated by the primary loop and the voltage induced in the small receiving loop, which are not subject to simplifying assumptions and are valid in a wide frequency range. The expressions are obtained starting from the decomposing the integral representation for the vertical magnetic field along the axis of the loops into three terms, that is the direct field, the ideal reflected field, and an additional correction term due to the imperfect conductivity of the ground. After making explicit the first two terms, a least squares-based fitting procedure is used to generate a

*Received 8 December 2020, Accepted 26 January 2021, Scheduled 29 January 2021*

* Corresponding author: Marcello Salis (marcello.salis@yahoo.it).

[1] Department of Industrial and Information Engineering and Economics, University of l'Aquila, L'Aquila, Italy. [2] Independent Researcher, Via Gregorio Ricci Curbastro 34, Rome 00149, Italy.

rational approximation, in pole-residue form, for the even part of the integrand of the correction term. This leads to turn the original integral describing the correction term into a sum of known and tabulated integrals. As a result, the vertical magnetic field and the voltage induced in the secondary loop are expressed as combinations of exponential functions and modified Bessel functions of the second kind.

## 2. THEORY

The problem under study is depicted in Fig. 1. A large transmitting circular loop and a co-axial small receiving loop are positioned at height $h$ and $d$, respectively, above an $N$-layer lossy ground. The dielectric permittivity, electric conductivity, and magnetic permeability of the $n$th layer of the medium are indicated with $\epsilon_n$, $\sigma_n$, and $\mu_n$. The primary loop, with radius $b$, carries the sinusoidal current $Ie^{j\omega t}$, and produces at the center of the secondary loop the vertical magnetic field [10, Eqs. (4.19), (4.88)]

$$H_z = \frac{Ib}{2}\int_0^\infty \left[e^{-u_0|h-d|} + \frac{Y_0-\hat{Y}_1}{Y_0+\hat{Y}_1}e^{-u_0(h+d)}\right]\frac{\lambda^2}{u_0}J_1(\lambda b)d\lambda \tag{1}$$

where $J_\nu(\xi)$ is the $\nu$th-order Bessel function, and

$$u_n{=}\sqrt{\lambda^2-k_n^2}, \qquad\qquad k_n^2{=}\omega^2\mu_n\epsilon_n - j\omega\mu_n\sigma_n, \tag{2}$$

while $Y_0$ and $\hat{Y}_1$ are, respectively, the intrinsic admittance of free-space (zeroth layer) [10, Eq. (4.21)] and the surface admittance at the air-ground interface [10, Eq. (4.23)]. The intrinsic admittance of the $n$th layer of the medium is given by $Y_n{=}u_n/(j\omega\mu_n)$ [10, Eq. (4.27)], and the surface admittance at the upper boundary of the $n$th layer may be obtained from the recurrence relation [10, Eq. (4.25)]

$$\hat{Y}_n = Y_n\frac{\hat{Y}_{n+1}+Y_n\tanh(u_nt_n)}{Y_n+\hat{Y}_{n+1}\tanh(u_nt_n)}, \qquad n{=}N{-}1,\ldots,1, \tag{3}$$

with $\hat{Y}_N{=}Y_N$, and where $t_1, t_2, \ldots, t_{N-1}$ are the thicknesses of the $N{-}1$ finite layers. The aim of this work is to derive explicit expressions for $H_z$ and the voltage induced in the receiving loop. To this goal, we notice that the fraction in the integrand of the second integral in Eq. (4) may be rewritten in the form

$$\frac{Y_0-\hat{Y}_1}{Y_0+\hat{Y}_1}{=}-1+\frac{2Y_0}{Y_0+\hat{Y}_1}{=}-1+\frac{2u_0}{u_0+j\omega\mu_0\hat{Y}_1} \tag{4}$$

which allows to decompose Eq. (4) into three terms, namely the direct field produced by the source loop, the reflected field due to an ideal negative image, and a correction term. It reads

$$H_z = H_z^{(d)}+H_z^{(r)}+H_z^{(c)} = \Phi\left(|h-d|\right) - \Phi\left(h+d\right) + Ib\int_0^\infty \frac{e^{-u_0(h+d)}}{u_0+j\omega\mu_0\hat{Y}_1}J_1(\lambda b)\lambda^2 d\lambda, \tag{5}$$

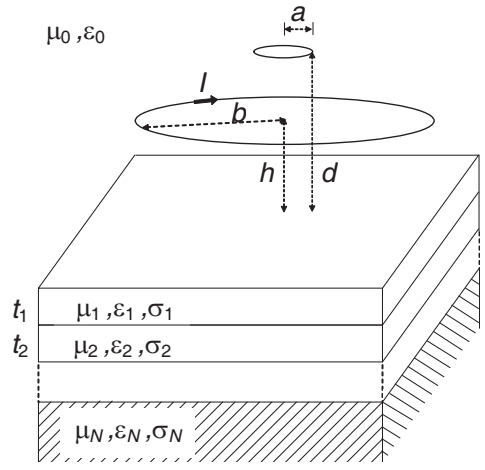


**Figure 1.** Two horizontal co-axial loops above a layered ground.

where the function $\Phi(\zeta)$ is known and given by [25]

$$\Phi\left(\zeta\right)=\frac{Ib}{2}\int_0^\infty\frac{e^{-u_0\zeta}}{u_0}J_1(\lambda b)\lambda^2 d\lambda=\frac{\left(1+jk_0r\right)Ib^2}{2r^3}e^{-jk_0r},\tag{6}$$

with $r{=}\sqrt{b^2+\zeta^2}$. The last integral on the right-hand side of Eq. (5) may be evaluated after expressing the fraction of the integrand, that is an even function of $\lambda$, in pole-residue form by means of a rational approximation. In particular, the well-known least squares-based fitting procedure described in [26] can provide the following representation [27, 28]

$$\frac{e^{-u_0(h+d)}}{u_0+j\omega\mu_0\hat{Y}_1}\cong\sum_{l=1}^{L}\frac{r_l}{j\lambda^2-p_l},\qquad\mathrm{Re}[p_l]<0,\tag{7}$$

with $L$ being the order of the approximation. In virtue of Eq. (7) and the differentiation properties of the Bessel functions, the last integral in Eq. (5) becomes

$$\int_0^\infty\frac{e^{-u_0(h+d)}}{u_0+j\omega\mu_0\hat{Y}_1}J_1(\lambda b)\lambda^2 d\lambda\cong-\sum_{l=1}^{L}r_l\frac{\partial}{\partial b}\int_0^\infty\frac{1}{j\lambda^2-p_l}J_0(\lambda b)\lambda d\lambda,\tag{8}$$

and after applying the identity [25]

$$\int_0^\infty\frac{1}{\lambda^2+\kappa^2}J_0(\lambda b)\lambda d\lambda=K_0(\kappa b)\tag{9}$$

with $K_0(\xi)$ being the zeroth-order modified Bessel function of the second kind, one obtains

$$\int_0^\infty\frac{e^{-u_0(h+d)}}{u_0+j\omega\mu_0\hat{Y}_1}J_1(\lambda b)\lambda^2 d\lambda\cong j\sum_{l=1}^{L}r_l\frac{\partial}{\partial b}K_0(\sqrt{jp_l}b)=-j\sum_{l=1}^{L}r_l\sqrt{jp_l}K_1(\sqrt{jp_l}b).\tag{10}$$

Finally, use of Eq. (10) together with Eq. (6) into Eq. (5) provides an explicit expression for the $H_z$-field, that is

$$H_z{=}\left.\frac{\left(1+jkr\right)Ib^2}{2\,r^3}e^{-jkr}\right|_{\zeta=h+d}^{\zeta=h-d}-jIb\sum_{l=1}^{L}r_l\sqrt{jp_l}K_1(\sqrt{jp_l}b),\tag{11}$$

and under the assumption that the receiving loop is both electrically and physically small (small loop approximation), the voltage induced in it may be expressed as [10]

$$V=j\omega\mu_0\pi a^2H_z{=}j\omega\mu_0\pi a^2\left[\left.\frac{\left(1+jkr\right)Ib^2}{2\,r^3}e^{-jkr}\right|_{\zeta=h+d}^{\zeta=h-d}-jIb\sum_{l=1}^{L}r_l\sqrt{jp_l}K_1(\sqrt{jp_l}b)\right].\tag{12}$$

## 3. NUMERICAL RESULTS

The validity of Eqs. (11) and (12) is tested through comparison of their outcomes with the data provided by Gaussian numerical integration of Eq. (1), performed by using Quadpack library contained in the Slatec mathematical libraries. First, the proposed expressions are used to calculate the amplitude-frequency spectra of the central vertical magnetic field and the voltage response of a source-receiver system placed on the surface of a two-layer soil ($h{=}d{=}0$), constituted by an alluvial fill, 4 m in thickness, covering a bedrock terrace ($\epsilon_1{=}\epsilon_2{=}10\,\epsilon_0$, $\sigma_1{=}100$ mS/m, $\sigma_2{=}1$ mS/m, $\mu_1{=}\mu_2{=}\mu_0$). The large source loop carries 1 A of current, and its radius is taken to be equal to 10 m. On the other hand, the radius of the small loop, co-planar and co-axial with the former, is 50 cm. The order $L$ of the approximation in Eq. (7) is taken as a parameter and, for any fixed value of it, the corresponding set of pole-residue pairs results from a procedure that consists of repeatedly applying the fitting algorithm in [26], until the root mean square (RMS) relative error of the approximation in Eq. (7) falls below the tolerance of $10^{-4}$. The results of the computation are depicted in Figs. 2 and 3, where, in particular, the induced voltage per unit current is referred to as the mutual impedance of the loops. The plotted curves show that, as

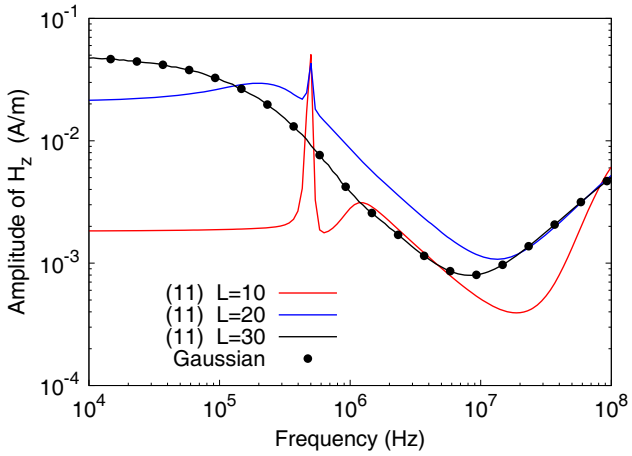


**Figure 2.** Amplitude of the vertical magnetic field against frequency.

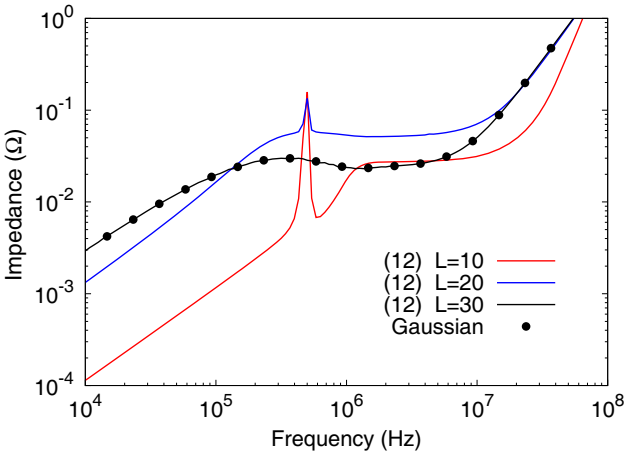


**Figure 3.** Mutual impedance of the two loops against frequency.

$L$ grows up, the frequency spectra arising from Eqs. (11) and (12) approach the corresponding trends provided by Gaussian quadrature, and that perfect agreement is obtained when $L$=30. Agreement is not obtained at the price of a considerable time cost. In fact, on a single-core 2 GHz processor, the average computation time taken by the fitting-algorithm described in [26] to generate the required 30 pole-residue pairs is slightly less than 3 s, while 7.6 s are taken by Gaussian quadrature of Eq. (1) to produce the results depicted in Fig. 2, and this implies that the proposed approach is advantageous in terms of time cost with respect to numerical integration procedures. Figs. 2 and 3 also tell us that for $L$<30 the proposed method does not succeed in providing sufficiently accurate results. This aspect is further investigated in Fig. 4, which illustrates the relative error of the outcomes of Eq. (11) plotted in Fig. 2, as compared to numerical integration data. As can be noticed, when $L$=22 or $L$=26 the relative error is in general non-negligible. In particular, it is higher than 10% in a wide frequency range, even if significant reductions are observed for frequencies higher than 1 MHz. Instead, when $L$=30 the error is almost always smaller than 1%, and beyond 1 MHz it dramatically decreases as frequency is increased, down to $10^{-6}$ at 10 MHz. It should be observed that increasing $L$ improves the computational accuracy because it breaks down the RMS relative error of the approximation in Eq. (7). In fact, repeated application of the algorithm in [26] allows to obtain average RMS errors equal to about $5.6 \cdot 10^{-5}$ for $L$=22, $7.4 \cdot 10^{-6}$ for $L$=26, and $3.2 \cdot 10^{-9}$ for $L$=30. This means that, for any considered value of $L$, we are able to approximately predict the final computational accuracy, by checking whether the corresponding RMS error of Eq. (7) is smaller than, comparable to, or larger than $10^{-9}$. Moreover, Fig. 4 also suggests that at lower frequencies and, hence, for smaller values of the wavenumbers, higher values of $L$ are required in order to minimize the RMS error of Eq. (7) and achieve accurate results. The same happens when the electrical conductivities of the layers are reduced, since the reduction leads to smaller values of the wavenumbers. Finally, Fig. 5 shows a set of theoretical response curves that may be used for interpreting previously recorded on-site measurements data. The curves come from applying Eq. (12) with $L$=30, under the hypothesis that the dimensions of the antennas and their positions are the same as in the previous example. Here, it is assumed that $\epsilon_1$=$\epsilon_2$=10$\epsilon_0$, $\sigma_1$=10 mS/m, $\mu_1$=$\mu_2$=$\mu_0$, and $d_1$=1 m, while the conductivity contrast $\sigma_2/\sigma_1$ is taken as a parameter, which is usually done to make it possible real data interpretation. As pointed out by the plotted curves, increasing the conductivity contrast has the effect of moving the amplitude-frequency spectrum of the mutual impedance between the source and the receiver downwards. In particular, a significant degree of dissimilarity is observed among the four plotted spectra of the mutual impedance, this implying good resolution of the EM sounding technique, which increases the chances to determine the real electrical conductivity of the bottom-most layer.

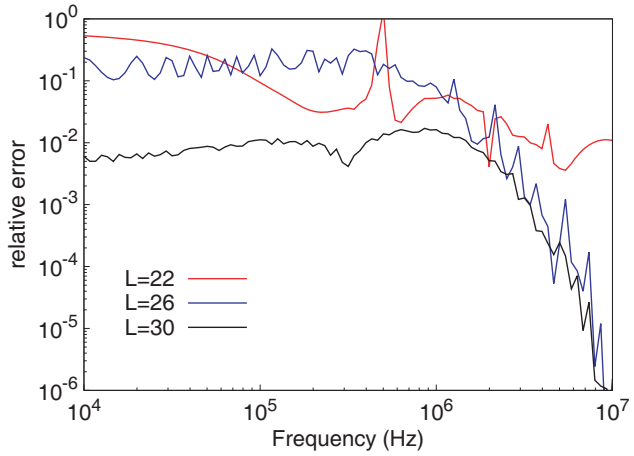


**Figure 4.** Relative error of (11) as compared to numerical integration.

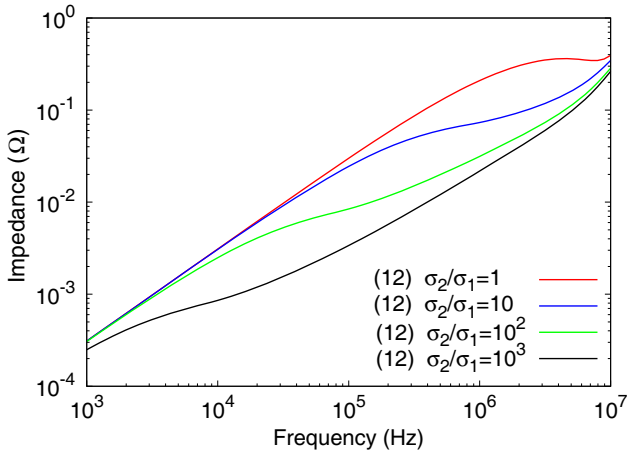


**Figure 5.** Mutual impedance against frequency, with $\sigma_2/\sigma_1$ taken as a parameter.

## 4. CONCLUSIONS

This work has presented a method for efficiently evaluating the time-harmonic vertical magnetic field produced at the center of a large loop antenna positioned above a layered ground. After extracting the direct and ideal reflected fields from the integral representation for the vertical magnetic field, the non-analytic part of the integrand of the remaining integral term has been replaced with a rational function obtained by using a well-known fitting algorithm. Then, the resulting sum of integrals has been converted into a sum of modified Bessel functions of the second kind. Performed numerical tests have confirmed that the obtained expression for the vertical magnetic field converges to the exact solution to the problem and that it is advantageous in terms of time cost over numerical integration procedures.

## REFERENCES

1. Boerner, D. E., "Controlled source electromagnetic deep sounding: Theory, results and correlation with natural source results," *Surveys in Geophysics*, Vol. 13, No. 4–5, 435–488, 1992.
2. Constable, S. C., R. L. Parker, and C. G. Constable, "Occam's inversion: A practical algorithm for generatlng smooth models from electromagnetic sounding data," *Geophysics*, Vol. 52, No. 3, 289–300, 1987.
3. Shastri, N. L. and H. P. Patra, "Multifrequency sounding results of laboratory simulated homogeneous and two-Layer earth models," *IEEE Trans. Geosci. Remote Sensing*, Vol. 26, No. 6, 749–752, 1988.
4. Parise, M., "Improved Babylonian square root algorithm-based analytical expressions for the surface-to-surface solution to the Sommerfeld half-space problem," *IEEE Transactions on Antennas and Propagation*, Vol. 63, 5832–5837, 2015.
5. Parise, M., "Exact EM field excited by a short horizontal wire antenna lying on a conducting soil," *AEU — International Journal of Electronics and Communications*, Vol. 70, No. 5, 676–680, 2016.
6. Farquharson, C. G., D. W. Oldenburg, and P. S. Routh, "Simultaneous 1D inversion of loop-loop electromagnetic data for magnetic susceptibility and electrical conductivity," *Geophysics*, Vol. 68, No. 6, 1857–1869, 2003.
7. Parise, M., "On the use of cloverleaf coils to induce therapeutic heating in tissues," *Journal of Electromagnetic Waves and Applications*, Vol. 25, No. 11–12, 1667–1677, 2011.
8. Romano, D., I. Kovacevic-Badstubner, M. Parise, U. Grossner, J. Ekman, and G. Antonini, "Rigorous dc solution of partial element equivalent circuit models including conductive, dielectric,

and magnetic materials," *IEEE Transactions on Electromagnetic Compatibility*, Vol. 62, No. 3, 870–879, 2020.

9. Beard, L. P. and J. E. Nyquist, "Simultaneous inversion of airborne electromagnetic data for resistivity and magnetic permeability," *Geophysics*, Vol. 63, No. 5, 1556–1564, 1998.
10. Ward, S. H. and G. W. Hohmann, "Electromagnetic theory for geophysical applications," *Electromagnetic Methods in Applied Geophysics, Theory — Volume 1*, 131–308, edited by M. N. Nabighian, SEG, Tulsa, Oklahoma, 1988.
11. Parise, M., "Second-order formulation for the quasi-static field from a vertical electric dipole on a lossy half-space," *Progress In Electromagnetics Research*, Vol. 136, 509–521, 2013.
12. Spies, B. R. and F. C. Frischknecht, "Electromagnetic sounding," *Electromagnetic Methods in Applied Geophysics, Volume 2*, 285–426, edited by M. N. Nabighian, SEG, Tulsa, Oklahoma, 1988.
13. Parise, M., L. Lombardi, F. Ferranti, and G. Antonini, "Magnetic coupling between coplanar filamentary coil antennas with uniform current," *IEEE Transactions on Electromagnetic Compatibility*, Vol. 62, 622–626, 2020.
14. Tiwari, K. C., D. Singh, and M. K. Arora, "Development of a model for detection and estimation of depth of shallow buried non-metallic landmine at microwave x-band frequency," *Progress In Electromagnetics Research*, Vol. 79, 225–250, 2008.
15. Parise, M., "An exact series representation for the EM field from a circular loop antenna on a lossy half-space," *IEEE Antennas and Wireless Prop. Letters*, Vol. 13, 23–26, 2014.
16. Werner, D. H., "An exact integration procedure for vector potentials of thin circular loop antennas," *IEEE Transactions on Antennas and Propagation*, Vol. 44, 157–165, 1996.
17. Parise, M., "Full-wave analytical explicit expressions for the surface fields of an electrically large horizontal circular loop antenna placed on a layered ground," *IET Microwaves, Antennas & Propagation*, Vol. 11, 929–934, 2017.
18. Palacky, G. J., "Resistivity characteristics of geologic targets," *Electromagnetic Methods in Applied Geophysics*, Vol. 1, 52–129, Nabighian, M. N., Ed., SEG, Tulsa, Oklahoma, 1988.
19. Singh, N. P. and T. Mogi, "Electromagnetic response of a large circular loop source on a layered earth: A new computation method," *Pure and Applied Geophysics*, Vol. 162, 181–200, 2005.
20. Parise, M., "Efficient computation of the surface fields of a horizontal magnetic dipole located at the air-ground interface," *International Journal of Numerical Modelling: Electronic Networks, Devices and Fields*, Vol. 29, 653–664, 2016.
21. Wait, J. R., "Fields of a horizontal loop antenna over a layered half-space," *Journal of Electromagnetic Waves and Applications*, Vol. 9, No. 10, 1301–1311, 1995.
22. Parise, M. and G. Antonini, "On the inductive coupling between two parallel thin-wire circular loop antennas," *IEEE Transactions on Electromagnetic Compatibility*, Vol. 60, 1865–1872, 2018.
23. Singh, N. P. and T. Mogi, "Effective skin depth of EM fields due to large circular loop and electric dipole sources," *Earth Planets Space*, Vol. 55, 301–313, 2003.
24. Parise, M., "An exact series representation for the EM field from a vertical electric dipole on an imperfectly conducting half-space," *Journal of Electromagnetic Waves and Applications*, Vol. 28, No. 8, 932–942, 2014.
25. Watson, G. N., *A treatise on the theory of Bessel functions*, Cambridge University Press, Cambridge (UK), 1944.
26. Gustavsen, B. and A. Semlyen, "Rational approximation of frequency domain responses by vector fitting," *IEEE Transactions on Power Delivery*, Vol. 14, 1052–1061, 1999.
27. Parise, M. and S. Cristina, "High-order electromagnetic modeling of shortwave inductive diathermy effects," *Progress In Electromagnetics Research*, Vol. 92, 235–253, 2009.
28. Parise, M., "A study on energetic efficiency of coil antennas used for RF diathermy," *IEEE Antennas and Wireless Propagation Letters*, Vol. 10, 385–388, 2011.